Pharm Res (2011) 28:3079–3090
DOI 10.1007/s11095-011-0547-x

RESEARCH PAPER

# MicroRNA-101 Inhibits Growth of Epithelial Ovarian Cancer by Relieving Chromatin-Mediated Transcriptional Repression of $p21^{waf1/cip1}$

Assaad Semaan • Aamer M. Qazi • Shelly Seward • Sreedhar Chamala • Christopher S. Bryant • Sanjeev Kumar • Robert Morris • Christopher P. Steffes • David L. Bouwman • Adnan R Munkarah • Donald W. Weaver • Scott A. Gruber • Ramesh B. Batchu

Received: 28 March 2011 / Accepted: 22 July 2011 / Published online: 5 August 2011


## ABSTRACT

***Purpose*** MicroRNA-101 (miR-101) expression is negatively associated with tumor growth and proliferation in several solid epithelial cancers. Enhancer of zeste homolog 2 (EzH2) appears to be a functional target of miR-101. We explore the role of miR-101 and its interaction with EzH2 in epithelial ovarian carcinoma (EOC).

***Methods*** *In situ* hybridization (ISH) for miR-101 was performed on EOC patient tissues and normal controls. EOC cell lines were transfected with miR-101 and subjected to growth analysis and clonogenic assays. Cell motility was assessed by Boyden chamber and wound-healing assays. $P21^{waf1/cip1}$ and EzH2 interaction was assessed by Chromatin Immunoprecipitation (ChIP) assay in MDAH-2774 cells. SCID mice were assessed for tumor burden after injection with miR-101 or control vector-treated MDAH-2774 cells.

***Results*** ISH analysis revealed a decrease in miR-101 expression in EOC compared with normal tissue. MiR-101 re-expression in EOC cell lines resulted in increased apoptosis, decreased cellular proliferation, invasiveness, and reduced growth of tumor xenografts. CHIP assays revealed that re-expression of miR-101 inhibited the interaction of EzH2 with $p21^{waf1/cip1}$ promoter.

***Conclusions*** MiR-101 re-expression appears to have antitumor effects, providing a better understanding of the role of miR-101 in EOC.

Assaad Semaan, Aamer M. Qazi, and Shelly Seward are equal contributors to the manuscript.

A. Semaan • A. M. Qazi • S. Seward • S. Chamala • C. P. Steffes • D. L. Bouwman • D. W. Weaver • R. B. Batchu
Laboratory of Surgical Oncology & Developmental Therapeutics
Department of Surgery, Wayne State University
Detroit, Michigan 48201, USA

A. Semaan • S. Seward • R. Morris
Department of Ob/Gyn, Wayne State University
Detroit, Michigan 48201, USA

C. S. Bryant
MD Anderson Cancer Center Orlando, Gynecologic Oncology
Orlando, Florida 32806, USA

S. Kumar
Division of Gynecologic Surgery, Mayo Clinic Cancer Center
Rochester, Minnesota 55905, USA

A. Semaan • A. M. Qazi • S. Seward • S. Chamala • R. Morris • C. P. Steffes • D. L. Bouwman • D. W. Weaver • S. A. Gruber • R. B. Batchu
John D. Dingell VA Medical Center
Detroit, Michigan 48201, USA

A. M. Qazi • C. P. Steffes • D. L. Bouwman • D. W. Weaver • R. B. Batchu
Karmanos Cancer Institute
Detroit, Michigan 48201, USA

A. R. Munkarah
Department of Women's Health Services, Henry Ford Health System
Detroit, Michigan 48202, USA

R. B. Batchu (✉)
Department of Surgery, Wayne State University
John D Dingell VA Medical Center
4646 John R Rd.
Detroit, Michigan 48201, USA
e-mail: rbatchu@med.wayne.edu

**KEY WORDS** enhancer of zeste homolog 2 (EzH2) · epithelial ovarian cancer (EOC) · microRNA-101miR-101 · $p21^{waf1/cip1}$ · RNA interference (RNAi)

## INTRODUCTION

The incidence of ovarian cancer in the United States ranks eighth among cancers (excluding skin cancer), but fifth in terms of age-adjusted mortality (1). In the mid-1990s, the introduction of Paclitaxel to platinum-based treatment significantly improved survival in ovarian cancer patients (2). Today, the combination of Carboplatin and Paclitaxel, in addition to optimal surgical tumor debulking, represents the standard of care in epithelial ovarian carcinoma (EOC) treatment. Although chemotherapy achieves a clinical response in most of the cases, recurrence remains a major problem due to the appearance of drug resistance from residual tumor cells (3). The absence of effective screening methods to detect early stage disease and the propensity of ovarian cancer cells to develop chemotherapy-resistant clones substantially decrease the five-year overall survival of ovarian cancer patients, underscoring the need for more effective therapies (4).

Micro RNAs (miRNAs) are 19 to 24 nucleotides long, non-coding, double-stranded RNA molecules that are abundantly expressed and regulate eukaryotic gene expression at the level of translation. They form an imperfect complement to a target mRNA resulting in the blockade of translation or degradation of the RNA transcript (5). They use the same intracellular machinery that short interfering RNAs (siRNAs) use to inhibit translation, but unlike siRNAs that are primarily exogenous in origin, miRNAs are encoded by the genome and produced specifically to regulate gene expression.

Recent studies have shown that miRNAs play a critical role in tumor cells by serving as either oncogenes or tumor suppressor genes (6). The role of miRNAs in human cancers is further supported by the fact that >50% of miRNA genes are located at fragile genomic loci that are frequently altered by deletions and amplifications (7). In EOC, it is estimated that roughly 37% of miRNA genes have alterations in the DNA copy number at genomic loci (8). Several studies identified abnormalities in miRNA expression that are unique to ovarian cancer due to either gain or loss of the gene copy number (9). Over-expression or under-expression of certain miRNAs have been shown to be specific for EOC (10).

Recent studies have described specific miRNAs, often referred to as "epi-miRNAs," that play a significant role in transcriptional gene silencing via epigenetic changes including DNA methylation and histone modification. MicroRNA-101 (miR-101) is a quintessential example of this phenomenon, regulating the cancer epigenome through direct inhibition of enhancer of zeste homolog 2 methyltransferase (EzH2). EzH2 is a catalytic subunit of the polycomb repressive complex 2 (PRC2), responsible for trimethylation of histone H3 on lysine 27 (H3K27me3) eventually leading to the silencing of several tumor suppressor genes. MiR-101 has been shown to negatively regulate the cancer epigenome by directly targeting EzH2 in prostate and bladder cancers, thus inhibiting tumor progression (11,12).

Although several recent studies have examined the role of miR-101 in various cancers, the molecular mechanism of miRNA-mediated gene regulation in EOC remains elusive. Our results show that the re-expression of miR-101 represents an efficient modality that can be used to impair cell proliferation and the invasive potential of EOC *in vitro* and reduction of tumor xenografts *in vivo*. Further, we provide evidence that miR-101 negatively regulates EzH2 by binding to its 3′-UTR, thus relieving EzH2-mediated chromatin repression leading to an increase in the expression of the tumor suppressor $p21^{waf1/cip1}$.

## MATERIALS AND METHODS

### Patients

Using departmental databases, we identified 15 patients with EOC treated at Wayne State University who underwent primary surgery with no prior chemotherapy or radiation therapy. We also identified 5 patients who underwent surgery for benign ovarian lesions as controls. This protocol was approved by an institutional review board and received a waiver of consent for review of archived material and medical record. A retrospective chart review was performed to retrieve surgical and pathological data. Surgical staging was determined based on the International Federation of Obstetrics and Gynecology (FIGO) criteria. Tumor grade was designated as low or high according to the M.D. Anderson grading criteria (13).

### *In Situ* Hybridization (ISH)

We performed non-radioactive ISH on paraffin tissue sections with a double DIG-labeled probe according to the manufacturer's instructions (Exiqon, Woburn, MA). Briefly, the sections were deparaffinized in xylene and then gradually rehydrated in decreasing concentrations of ethanol. Sections were treated with proteinase K and then fixed with para-formaldehyde. Pre-hybridization was then carried out for 2 h in hybridization buffer (50% formamide, 5xSSC, 0.1%Tween, 9.2 mM citric acid for adjustment to a

pH of 6, 50 μg/mL heparin, 500 μg/mL yeast RNA) in a humidified chamber at 47°C. Slides were incubated in the DIG-labeled probe (containing miR-101 with the following sequence: 5′-TTC AGT TAT CAC AGT ACT GTA-3′) diluted to 25 nM in hybridization buffer overnight at 47°C. A stringency wash was then performed by rinsing slides in 2 × SCC, and the slides were placed in blocking buffer (2% sheep serum, 2 mg/mL BSA in PBST) for 1 h at room temperature. Immunological detection was performed using the DIG Nucleic Acid Detection Kit (Roche Diagnostics, Inc., Indianapolis, IN) according to the manufacturer's directions. Anti-DIG-AP conjugated antibody was diluted to 1:500 in blocking buffer and incubated overnight in a humidified chamber at 4°C. Nitro-blue tetrazolium (NBT) and 5-bromo-4-chloro-3-indolyl phosphate (BCIP) were used as chromogens. Slides were then rinsed in TE buffer (10 mM Tris-HCL/1 mM EDTA, pH 8) and mounted using the Aqua-Mount medium (Fisher, Houston, TX). The slides were then examined under a transmission light microscope. Staining intensity was scored as 0 (negative), 1 + (weak), 2 + (medium) or 3 + (strong). Low expression was defined as an intensity of 0, 1, 2, or 3 and <10% stained cells or an intensity of 0 or 1 and <50% stained cells. High expression was defined as an intensity of 2 or 3 and >10% stained cells, or an intensity of 1, 2, or 3 and >50% stained cells.

### Reagents and Antibodies

All reagents, unless specified, were from Sigma Chemical Co, St. Louis, USA. Pre-miR-101 expression vector is a micro-RNA construct (pMIR101-1PA-1 human) obtained commercially from System Bioscience (Mountain View, CA) with the following sequence: 5′-TGC CCT GGC TCA GTT ATC ACA GTG CTG ATG CTG TCT ATT CTA AAG GTA CAG TAC TGT GAT AAC TGA AGG ATG GCA-3′, expressed from a CMV promoter. A fluorescent marker (GFP) is also present to monitor cells that are positive for transfection. For the control vector, we used the same vector without the pre-miR-101 sequence. EzH2, $p21^{waf1/cip1}$, and H3K27 antibodies were purchased from Millipore (Danvers, MA). Cyclins, CDKs, poly (ADP-ribose) polymerase (PARP) and β actin and other apoptosis-related antibodies were purchased from Santa Cruz Biotechnology, (Santa Cruz, CA).

### Cell Lines and Culture

EOC cell lines MDAH-2774, SKOV-3 and TOV-21G (American Type Culture Collection, Manassas, VA) were propagated in McCoy's 5A medium supplemented with 10% fetal bovine serum, 2 mM L-glutamine, and antibiotics (Thermo Fisher Scientific, Pittsburgh, PA). Cells were cultured in a humidified atmosphere with 5% $CO_2$ at 37°C. Trypsin (0.25%)/EDTA solution was used to detach the cells from the culture flask. Normal human ovarian surface epithelial cells (HOSEpiC) were purchased and maintained in ovarian surface epithelial cell medium from ScienCell Research Laboratories (Calsbad, CA.) as recommended by the manufacturer.

### RT-PCR Quantification of MiR-101 in Cell Lines

Briefly, total RNA was extracted from tissues and cells using Trizol (Invitrogen, Carlsbad, CA). cDNA synthesis was carried out with the Superscript III cDNA synthesis kit (Invitrogen, Carlsbad, CA) according to the manufacturer's instructions. The resulting cDNA was amplified with miR-101 primers; 5′-TGG GCT ACA GTA CTG TGA TA-3′ and 5′-TGC GTG TCG TGG AGT C-3′ with 93°C for 4 min, followed by 35 cycles of 93°C for 10 s, 60°C for 20 s and 72°C for 20 s. At the end of the PCR cycles, melting curve analysis was performed. The baseline expression of miR-101 in ovarian cancer cell lines was compared to the miR-101 level in HOSEpiC cells. MiR-101 levels were also checked before and after transfection with miR-101 or control vector in TOV-21G, MDAH-2774 and SKOV-3 cell lines relative to the miR-101 level in control vector transfected TOV-21G cells.

### Cell Proliferation Assays

Standard prototype growth curves and number of viable cells were determined for each cell line (treated and control groups) in triplicate experiments according to the CCK-8 (Dojindo, Gaithersburg, MD) manufacturer's instructions. Growth curves were plotted as a percentage of the value of DMSO-treated controls minus the value of untreated cells on day 0. Day 3 values were considered for the determination of the 50% cell proliferation inhibition (IC50) for a given treatment. In some cases, a parallel manual count was also performed with trypan blue and counting by exclusion method using a hemocytometer. The findings confirmed CCK-8 assay results.

### Colony Formation Assay

MDAH-2774, SKOV-3, and TOV-21G cells were transfected with either miR-101 or control vector using the Effectene reagent (Qiagen, Valencia, CA). Transfected cells were trypsinized after 48 h and seeded at a concentration of 1,000 cells per well in 6-well plates containing McCoy's 5A supplemented with 10% FBS. The assay was done in triplicate. After incubation for 14 days, the cells were washed and fixed in absolute methanol for 15 min at −20°C and stained with crystal violet in 25% methanol. The colonies were then counted, photographed, and quantified using the

ImageJ software (Java-based image processing program, a public domain developed at the National Institutes of Health).

### Analysis of Apoptotic Cells

The apoptosis assay was performed using the annexin V-FITC apoptosis detection Kit I (Calbiochem, Gibbstown, NJ) according to the manufacturer's instructions. Briefly, MDAH-2774 and SKOV-3 cells were transfected with miR-101 or a control vector and allowed to grow for 48 h. Both floating and non-floating cells were collected by trypsinization, washed twice in PBS, and re-suspended in Annexin-V binding buffer at a concentration of $10^6$ cells/ml. An aliquot of 100 µl of this suspension was stained with 5 µl of Annexin-V-FITC and 5 µl of propidium iodide (PI) and incubated for 15 min at room temperature in the dark. Subsequently, the DNA content of the sub G1 cell population, representing apoptotic cells, was suspended in 400 µl of binding buffer and subjected to fluorescence-activated cell sorting (FACS) analysis.

### *In Vitro* Invasion and Wound-Healing Assays

The cell invasion assay was performed with a modified Boyden chamber using filters with a pore size of 8-µm. Briefly, miR-101 transfected MDAH-2774 ($10^5$/500 µL) were added to the upper chamber with the lower chamber filled with medium and incubated for 18 h at 37°C in a 5% $CO_2$ humidified chamber. Cells on the upper surface of the membrane were then removed using wet cotton swabs. The underside of the membrane was washed twice with PBS and stained with 4 µM Calcein stain (Invitrogen, Carlsbad, CA). The migrated cells on the membrane side facing the bottom chamber were counted under a fluorescent microscope in five random fields (x200), and the average value was calculated. For wound-healing assays, miR-101 and control vector transfected MDAH-2774 cells were plated at an equal density and grown to 80% confluence. Monolayer cells were disrupted mechanically with a pipette tip to generate a wound ridge free of cells, and the extent of cell migration, as measured by their ability to close the artificially created gap, was documented under a light microscope.

### Western Blotting

Proteins were separated using 4–15% SDS Tris-Glycine gels and western transfer of proteins to nitrocellulose papers was conducted with iBlot dry blotting device (InVitrogen Corp, Carlsbad, CA). Blocking agent was 3% nonfat milk powder and secondary antibodies were conjugated to HRPO (Santa Cruz Biotechnology, Santa Cruz, CA). Antibody reactions were visualized using enhanced chemiluminescence western blotting detection reagents (Amersham Pharmacia, Uppsala, Sweden).

### Chromatin Immunoprecipitation (ChIP) Assay

The ChIP assay was performed using the Chromatin Immunoprecipitation Assay kit (EZ-Magna ChIPTM A, Cat # 17-408, Upstate, Temecula, CA), according to the manufacturer's instructions. Briefly, $1\times10^7$ MDAH-2774 cells were transfected with miR-101 or the control vector. After 48 h, 1% formaldehyde was added to the cells for 10 min at 25°C. Cells were harvested, lysed, and sonicated ($8\times15$ s with 50 s cooling). The soluble chromatin was then immunoprecipitated with anti-EzH2 (Cat # 07-689, Millipore, Billerica, MA). DNA–protein immune complexes were eluted and reverse cross-linked, and the DNA was extracted using a spin filter column. Standard end-point PCR was performed using JumpStart REDTaq PCR mix (Cat # P 0982, Sigma, Saint Louis, Missouri). The presence of the $p21^{waf1/cip1}$ promoter domain in immunoprecipitated DNA was identified by using the following primers: forward primer 5′-GGT GTC TAG GTG CTC CAG GT-3′ and reverse primer 5′-GCA CTC TCC AGG AGG ACA CA-3′. The optimal reaction conditions were determined for PCR primers. Parameters were denaturation at 94°C for 1 min and annealing at 59°C for 1 min, followed by elongation at 68°C for 2 min. The amplified $p21^{waf1/cip1}$ promoter region targeting the −93 region from the transcriptional start site was analyzed after 30 cycles on 1% agarose/ethedium bromide gel electrophoresis showing a 255 bp band. In control samples, the primary antibodies were replaced with non-immune rabbit IgG.

### Luciferase MiR-101 Target Reporter Assay

The 3′UTR of EzH2 containing three intact miR-101 recognition sequences was amplified, and the PCR product was sub-cloned into a pGL3 vector (Promega Corporation, Madison WI) immediately downstream of the luciferase gene to generate pGL3-EzH2. pGL3-EzH2 constructs and miR-101 were transfected into SKOV-3 cells either alone or in combination. The luciferase activity assay was performed 24 h after transfection using the dual-luciferase reporter assay system (Promega Corporation, Madison WI).

### *In Vivo* Xenografts Tumorigenesis Studies

Six-week-old male CB17/Cr-SCID mice were obtained from Taconic Farms (Germantown, NY) and maintained under pathogen-free conditions. MDAH-2774 cells ($10^7$) transfected with miR-101 or control vector were suspended in 100 µl of PBS before being injected subcutaneously into the flanks of the experimental mice. Mice were randomized into two groups ($N=7$ for each group): control and miR-101. Once the tumors grew to a palpable size, approximately 10 days after injection, tumor diameters were

measured every 3 days for a total period of 50 days using digital calipers following a cutaneous shave of the tumor area. Tumor volume in $mm^3$ was calculated using the following formula: $(L \times W^2)/2$, where L is the maximum length and W is the maximum width of the tumor. At the end of the experiment, mice were euthanized and tumors harvested. The miR-101 level of tumors was also determined using RT-qPCR method described previously. All animal experiments included in this study were done in compliance with the institutional animal care and use committee (IACUC)/Wayne State University institutional guidelines (Protocol approval # A 12-06-07; animal investigation committee, 101 E. Alexandrine St., Detroit, MI).

### Statistical Analysis

Student's unpaired t-test was employed to evaluate the difference between the two groups. Data were expressed as the mean ± s.d. from at least three independent experiments. All p values were two-sided, and a value of $<0.05$ was considered to be statistically significant. Statistical analyses were performed with the SPSS for Windows (version 18.0; SPSS Inc, Chicago, Ill).

## RESULTS

### Expression of MiR-101 Down-Regulated in Tumor Tissue and Ovarian Cancer Cell Lines, Forced Re-expression Leads to Cell Proliferation Inhibition

To examine the clinical relevance of miR-101 in EOC, its expression was analyzed by ISH in normal control and in EOC patient tissues (Fig. 1a) (Table I). All normal ovarian tissues exhibited high miR-101 staining as compared to 33% in EOC tissues ($p=0.03$). In EOC patient tissue samples, a low miR-101 expression correlated with higher FIGO stage (III and IV) ($p=0.002$) but not with tumor grade ($p=0.5$).

We also examined the miR-101 expression in ovarian cancer cell linesTOV-21G, MDAH-2774, and SKOV-3 along with the non-malignant ovarian epithelial cell line HOSEpiC. As shown in Fig. 1b, ovarian cancer cell lines expressed lower levels of miR-101 compared with HOSEpiC cells. The level of miR-101 in ovarian cancer cells transfected with miR-101 or control vector was also evaluated. As shown in Fig. 1c, the miR-101 levels of control vector transfected cells were much lower than that of the miR-101 transfected cells.

Next, we addressed the question of whether forced expression of miR-101 could inhibit EOC growth and proliferation. MDAH-2774, SKOV-3 and TOV-21G cell lines were transfected with miR-101 or control vector, and cell growth was monitored over a period of 5 days. We observed a significant inhibition in cell proliferation in all three cell lines by day 5 as seen in Fig. 2a and b. MDAH-2774, SKOV-3, and TOV-21G cell lines had a 73%, 82%, and 77% reduction in the number of live cells compared to the baseline growth of control vector transfected cells, respectively. We further analyzed the long-term effect of miR-101 re-expression by performing clonogenic assays. MDAH-2774 cells were more firmly attached to the culture plates after transfection as compared to SKOV-3 and TOV-21G cells. However, all three cell lines (MDAH-2774, SKOV-3, and TOV-21G) had a significant decrease in the number and size of the colonies formed after transfection with miR-101 (Fig. 2c and d).

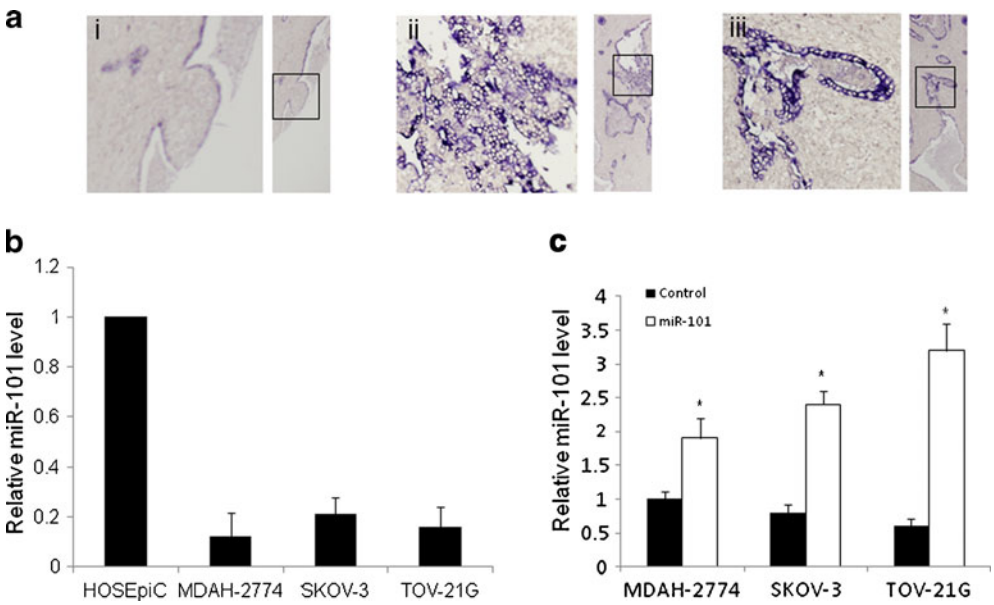


**Fig. 1** *In-situ* hybridization for miR-101 in tumor tissues and miR-101 levels in ovarian cancer cell lines. (**a**) *In situ* hybridization for miR-101 in stage IV EOC (i), stage IA EOC (ii), and normal ovarian tissue (iii). (**b**) Relative expression of miR-101 in ovarian cancer cell lines compared to human ovarian surface epithelial (HOSEpiC) cells. (**c**) Relative expression of miR-101 in control vector or pre-miR-101 transfected ovarian cancer cell lines compared to control vector transfected MDAH-2774 cells. $*p<0.05$.

**Table 1** Clinical Data and Tumor Pathology of Epithelial Ovarian Cancer Tissues

| Specimen/tissue control # | Age (Years) | Stage[a] | Grade | miR-101 staining |
|---|---|---|---|---|
| Case No. 1 | 58 | IA | Low | High |
| Case No. 2 | 71 | IIIA | Low | Low |
| Case No. 3 | 42 | IC | High | High |
| Case No. 4 | 65 | IIIC | High | Low |
| Case No. 5 | 68 | IV | High | Low |
| Case No. 6 | 28 | IC | High | High |
| Case No. 7 | 68 | IIB | High | High |
| Case No. 8 | 55 | IIIC | High | Low |
| Case No. 9 | 81 | IV | High | Low |
| Case No. 10 | 40 | IB | Low | High |
| Case No. 11 | 63 | IIA | Low | Low |
| Case No. 12 | 52 | IV | High | Low |
| Case No. 13 | 68 | IIIC | High | Low |
| Case No. 14 | 57 | IIIB | High | Low |
| Case No. 15 | 44 | IIIC | High | Low |
| Control No.1 | 54 | N/A | N/A | High |
| Control No.2 | 46 | N/A | N/A | High |
| Control No.3 | 69 | N/A | N/A | High |
| Control No.4 | 74 | N/A | N/A | High |
| Control No.5 | 50 | N/A | N/A | High |

Patient data in tissue sections used for *in situ* hybridization

[a]International federation for genecology and obstetrics (FIGO) staging

## Restoration of MiR-101 Expression Leads to Cell Motility and Invasiveness Inhibition

Cell invasion and migration are important *in vitro* measures of the metastatic potential of cancer cells. We observed that the transfection of pre-miR-101 expression plasmid resulted in a significant decrease in cell motility in MDAH-2774 cells (Fig. 3a). Further, we observed that miR-101 expression led to a ten-fold reduction in the invasive properties of these cells in Boyden chamber assay (Fig. 3b).

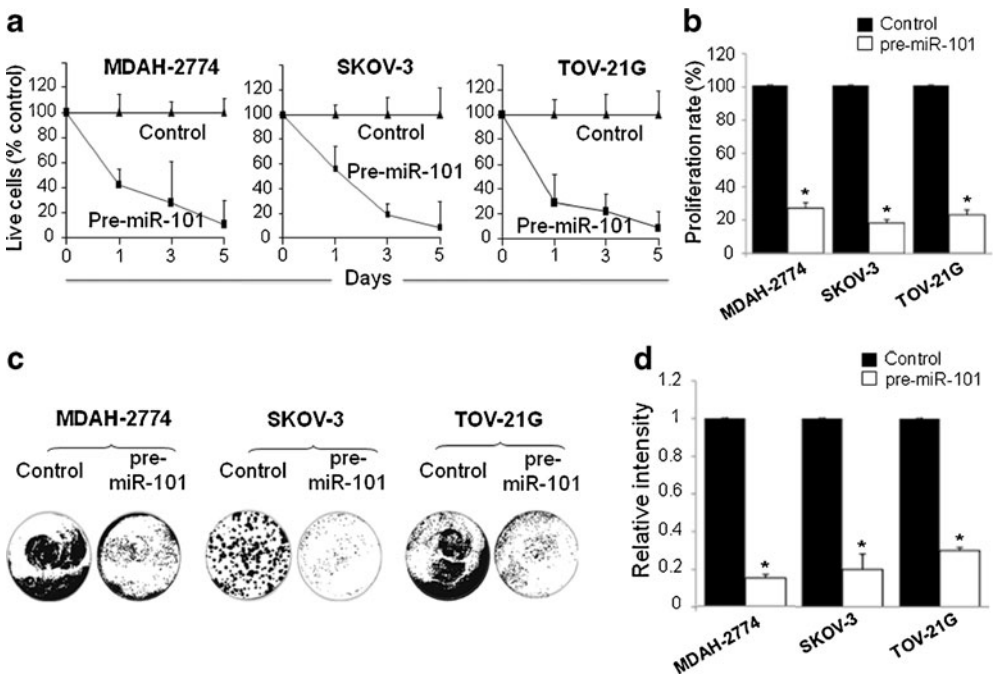


**Fig. 2** Cell growth and colony formation. (**a**) Cell growth inhibition by miR-101 re-expression in MDAH-2774, SKOV-3 and TOV-21G cells. (**b**) Values are expressed as percentage of proliferation on day 5 normalized to cells transfected with the control vector (set to 100%) from three separate experiments. (**c**) Representative pictures of the stained colonies are shown. (**d**) The number of colonies is expressed as relative intensity (measured by Image j program) normalized to cells transfected with the control vector (set to 100%) from three separate experiments. $^{*}P < 0.05$.

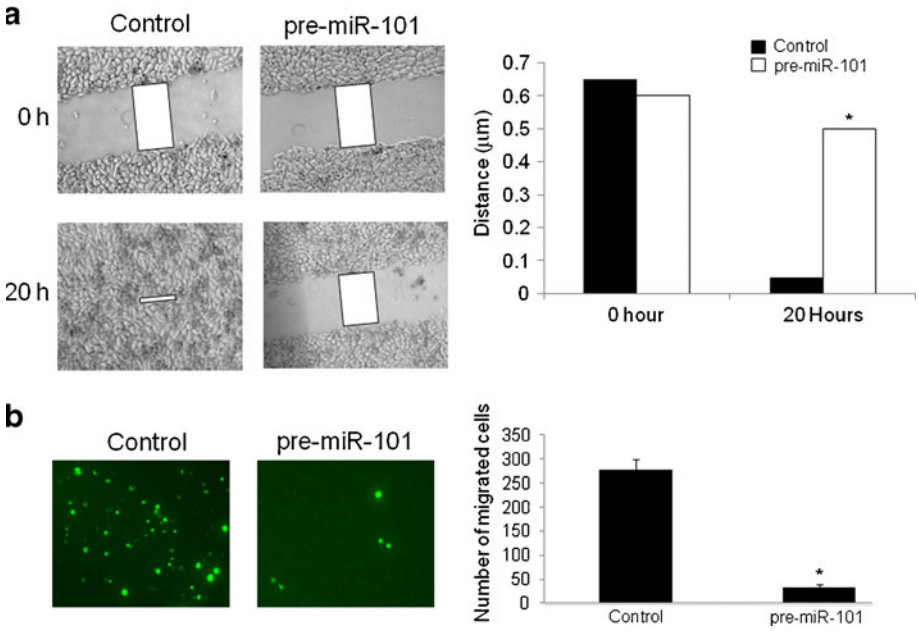


**Fig. 3** The effect of miR-101 re-expression on epithelial ovarian cancer cell invasiveness. (**a**) Wound-healing assay in MDAH-2774 cells: the extent of closure of the wound (cell migration) was monitored under phase-contrast microscopy, and photographs were taken at 0 and 20 h. The p value was compared to the control vector (*$p < 0.05$), and results represented the mean of two independent experiments in triplicates. (**b**) Trans-well migration assay in Boyden chamber using MDAH-2774 cells: average migrated cell number from three separate experiments. *$P < 0.05$.

## MiR-101-Induced Apoptosis in Ovarian Cancer Cells

FACS analysis was performed with PI and annexin V staining to determine whether miR-101 induces apoptosis in ovarian cancer cells. The percentage of pre-apoptotic cells increased by roughly 20% in response to miR-101 transfection in both MDAH-2774 an SKOV-3 cell lines (Fig. 4a). The percentage of post-apoptotic cells was significantly higher in slow-growing SKOV-3 cells compared with MDAH-2774 cells (18% and 11.1% respectively). As the balance between pro- and anti-apoptotic signals decides the fate of cells, we also examined the expression levels of genes involved in the apoptotic pathway by western blot analysis in MDAH-2774 and SKOV-3 cells after transfection with pre-miR-101. Forty-eight hours after transfection, we observed a significant increase in the expression of pro-apoptotic *bak* and anti-apoptotic *bcl-2* and a cleavage of PARP (known to be associated with activation of the intrinsic apoptotic pathway) in both cell lines (Fig. 4b).

## EzH2 is Direct and Functional Target of MiR-101

In order to identify miR-101 targets in humans, we conducted *in silico* analysis using the search program PicTar33. Among those predicted, two genes (EzH2 and COX-2) were identified as targets of miR-101 in other cancers including bladder, breast, and prostate carcinoma (14–17). We then evaluated the ability of miR-101 to regulate the 3′ UTR untranslated region of EzH2 in EOC by conducting luciferase reporter assays. Three putative binding sites of miR-101 were computationally determined in the 3′-UTR of the EzH2 promoter region using the PicTar33 software (Fig. 5a) (18). The 3′UTR target sites of EzH2 were cloned into a pGL3-vector, downstream of a luciferase gene. SKOV-3 cells were co-transfected with both pGL3-EzH2-luciferase vector and pre-miR-101. We found significantly lower levels of luciferase activity when the SKOV-3 cells were co-transfected with pre-miR-101 and pGL3-EzH2 luciferase vector (Fig. 5b). Hence, EzH2 seems to be a key downstream effector of miR-101 in EOC. We further investigated whether the ability of miR-101 to regulate the EzH2 3′UTR reflected on the endogenous EzH2 protein level. We observed a significant reduction in EzH2 protein level on western blot in MDAH-2774, SKOV-3 and TOV-21 cells transfected with pre-miR-101 (Fig. 5c).

## EzH2 Binding to $P21^{waf1/cip1}$ Promoter Modulated by MiR-101

Earlier results clearly established EzH2 as a downstream effector molecule for miR-101. In addition, it has been shown that EzH2 knockdown inhibits trimethylation of histone H3k27, enhancing the formation of inactive heterochromatin (19). Often, H3k27 trimethylation is observed at tumor suppressor genes, rendering them inaccessible for the transcriptional machinery and thus inhibiting their expression. This was confirmed in our study, as EzH2 knockdown in MDAH-2774 cells by miR-101 transfection resulted in a decrease in H3k27me3 levels (Fig. 6a).

Since miR-101 depletion leads to the over-expression of EzH2, a potent inhibitor of tumor suppressor genes, one might wonder whether some of the growth-inhibitory effects of miR-101 in EOC are due to re-expression of a

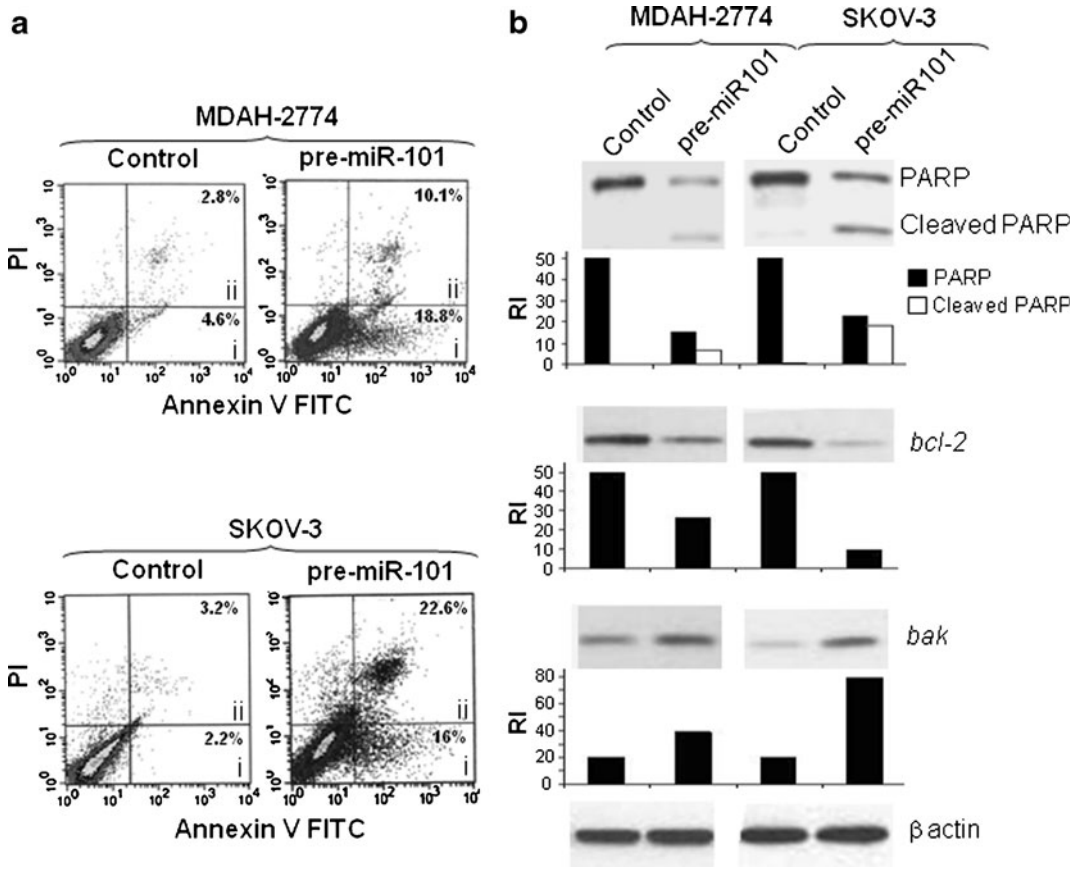


**Fig. 4** Effect of miR-101 re-expression on apoptosis. (**a**) MDAH-2774 and SKOV-3 cells ($1 \times 10^5$) were fixed, stained with annexin V FITC and propidium iodide (PI) (20 $\mu$g/ml), and subjected to FACS analysis. (**b**) Western blot analysis of poly (ADP-ribose) polymerase (PARP) protein, *bak*, *bcl-2* and β-actin in pre-miR-101 and control vector transfected MDAH-2774 and SKOV-3 cells. RI: relative intensity of the bands.

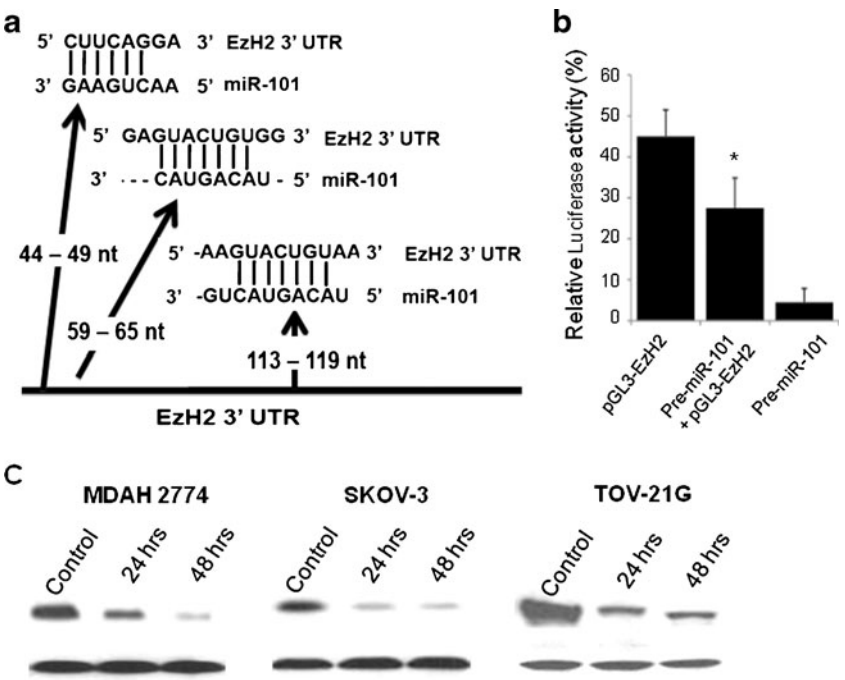


**Fig. 5** Validation of EzH2 as a target for miR-101 in epithelial ovarian cancer cells. (**a**) Three putative binding sites of miR-101 were computationally determined in the 3′-UTR of the EzH2 promoter region. (**b**) Luciferase activity was measured after 48 h and normalized against β-galactosidase values. Data are means ± S.D. of separate transfections ($n = 3$) and are shown as the ratio of firefly luciferase activity to β-galactosidase activity. Percentage of relative luciferase activity (*RLU*) was plotted. P value was compared to the control vector (*$p < 0.05$). (**c**) Western blot analysis of EzH2 expression in miR-101 and control vector transfected cells.

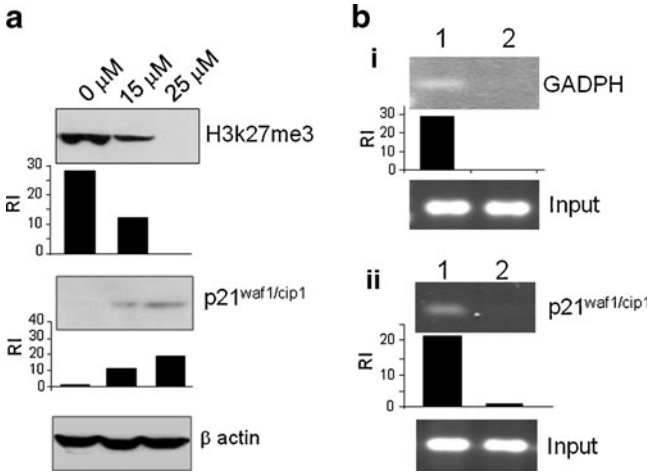


**Fig. 6** Influence of miR-101 re-expression on EzH2 interaction with the $p21^{waf1/cip1}$ promoter, the expression of p21 and H3k27me3. (**a**) MDAH-2774 cells were transfected with different concentrations of the miR-101 vector or the control vector. H3k27me3 and $p21^{waf1/cip1}$ expression was then evaluated by western blot analysis. RI: relative intensity of the bands. (**b**) Chromatin immunoprecipitation (ChIP) assay showing the binding of EzH2 to the $p21^{waf1/cip1}$ promoter region in the presence of miR-101 in MDAH-2774 cells. (i) In upper panel, GADPH primers were used as a positive control with Anti-acetyl Histone H3 as the immuno-precipitating antibody (lane 1). The same primers were used with the normal Rabbit IgG antibody as a negative control (lane 2). Lower panel shows equal loading using β-actin antibody. (ii) Upper panel shows ChIP assay performed in control vector (lane 1) and miR-101 transfected MDAH-2774 cells (lane 2) using anti-EzH2 antibody and $p21^{waf1/cip1}$ primers. A 255 bp band is shown targeting the −93 promoter region of $p21^{waf1/cip1}$ after performing a standard PCR reaction. Lower panel shows equal loading using β-actin antibody. RI: relative intensity of the bands.

tumor suppressor genes. The tumor suppressor gene $p21^{waf1/cip1}$ is located on chromosome 6p21.2, which is prone to loss of heterozygosity in EOC (20). In addition, earlier studies indicated that the deregulation of $p21^{waf1/cip1}$ could provide a growth advantage in EOC (21). Based on these observations, we assessed the effect of miR-101 restoration on $p21^{waf1/cip1}$ expression. Western blot analysis in MDAH-2774 cells showed a significant increase in $p21^{waf1/cip1}$ levels (Fig. 6a). We then tested the level of $p21^{waf1/cip1}$ promoter occupancy by EzH2 protein, before and after its knockdown by miR-101 by chromatin immunoprecipitation (ChIP) assays in MDAH-2774 cells. The ChIP assays were carried out using anti-EzH2 and anti-β actin antibodies. Results not only indicated an interaction of EzH2 with $p21^{waf1/cip1}$ promoter, but also showed significantly decreased interaction when transfected with pre-miR-101 (Fig. 6b).

### Inhibition of Growth of Tumor Xenografts with Restoration of MiR-101 Expression

To evaluate the effect of restored miR-101 expression *in vivo*, MDAH-2774 cells were transfected with miR-101 or a control vector and then tested for their ability to form tumors. The tumor diameters were measured and tumor volumes calculated. Tumor xenografts formed by cells transfected with miR-101 were significantly smaller than control tumors throughout the study period of 50 days (Fig. 7a). The mean total tumor volume was $209 \pm 18$ $mm^3$ in the control group compared to $116 \pm 8$ $mm^3$ in the miR-101 transfected group ($p < 0.05$) (Fig. 7b). The expression of miR-101 in control vector injected tumors was much lower than that in miR-101 injected tumors ($1.12 \pm 0.23$ *versus* $1.54 \pm 0.15$, $P < 0.01$) (Fig. 7c).

## DISCUSSION

The discovery of miRNAs has broadened our understanding of carcinogenesis and has added an entirely new gene silencing modality. MiRNA alterations have been linked not only to the initiation and progression of cancer (22) but have also been associated with negative prognostic factors and response to treatment (23). Aberrant expression of miRNAs in human cancers is common, and often these miRNAs are referred to as oncomirs (24). Accumulating evidence points to a central regulatory role for miRNAs in the initiation and progression of most solid epithelial cancers analyzed so far. MiRNA profiling in EOC has only recently started, and the significance of alterations in different miRNA levels is largely unknown (10,25–28). For example, alteration in the expression of miR-214, miR-199a, miR-200a, and miR-100 have been reported in late-stage ovarian cancers (27).

MiRNAs in general have a broad specificity, as they do not require a perfect match with the complementary sequence of their target mRNA to silence the expression of a wide array of genes. The fact that miR-101 has been shown to silence the expression of several tumor promoting genes in the recent past, such as COX-2 in colon cancer (29), PKCα in hepatomas (30), and EzH2 in prostate cancer (17), suggests that the loss of expression of miR-101 might be a mark of solid tumor progression. Even though the role of miR-101 has been extensively studied in several solid epithelial malignancies, relatively little is known about its involvement in the progression of ovarian cancer.

In recent years, the loss of miR-101 expression was found to lead to the over-expression of EzH2, a pro-metastasic gene in prostate cancer (12,31) and transitional cell cancer of the bladder (11). In prostate cancer, progressive decrease in miR-101 levels was correlated with an increase in the expression of EzH2, paralleled by an increase in the metastatic potential of cancer cells (12). In our study, we report that miR-101 negatively regulates EzH2 in EOC cell lines by binding to its 3′-UTR, leading to inhibition of translation. Over-expression of miR-101,

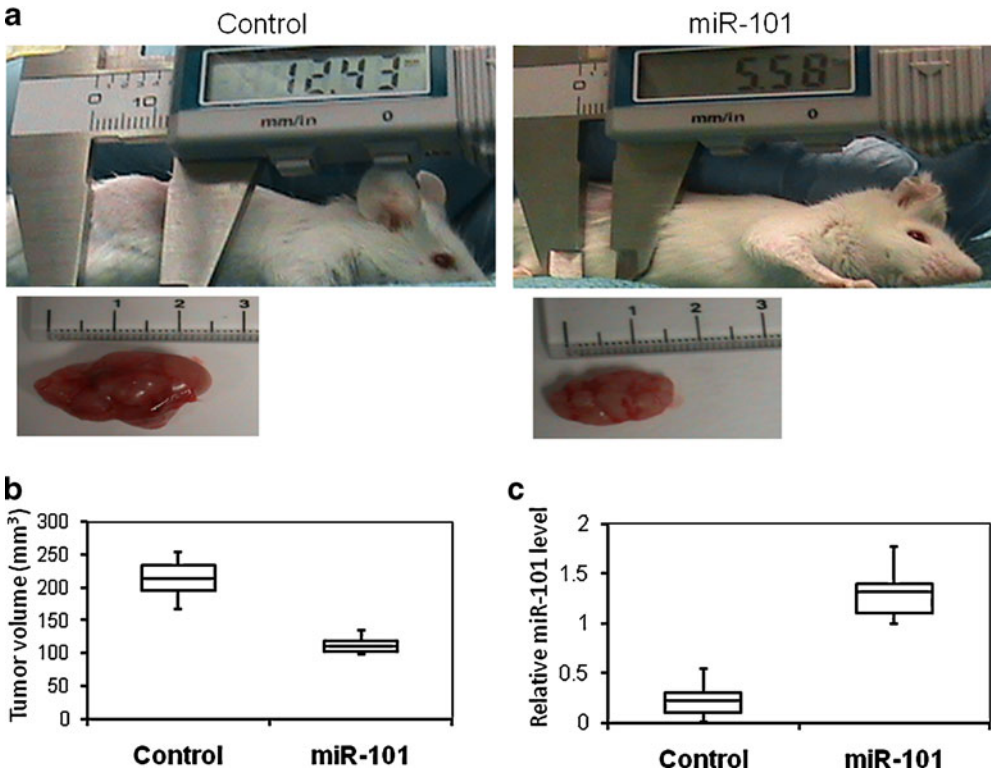


**Fig. 7** Influence of miR-101 re-expression on tumor xenograft growth in mice. (**a**) Xenografts of miR-101 and control vector transfected MDAH-2774 cells in SCID mice. (**b**) Average volume of tumors harvested. (**c**) Relative expression of miR-101 in control vector or pre-miR-101 injected tumors compared to that in one control vector injected tumor.

but not the control vector, decreased the activity of the luciferase reporter encoding the 3′ UTR of EzH2. These observations corroborate the idea that the loss of miR-101 might be a signature of solid epithelial carcinomas.

Our ISH results confirm that miR-101 is less abundant in EOC patient tissues as compared to normal ovarian tissue. In addition, low levels of miR-101 strongly correlated with FIGO stage but not with tumor grade. This might be due to the small sample size, since only 4 of the 15 patients with EOC included in the study had low-grade tumors. These observations are an eye opener to the role of miR-101 re-expression as a potential therapeutic intervention in EOC.

As a catalytic subunit of the PcG complex, the EzH2 protein complex's primary activity is to trimethylate histone H3K27 in the promoter areas of target tumor suppressor genes leading to epigenetic silencing of those genes by chromatin restructuring. Based on this observation, we reasoned that EzH2 depletion would negate this catalytic activity. In bladder transitional cell carcinoma, where EzH2 is down-regulated, H3K27me3 expression was also shown to be repressed (11). Our results confirm this observation, as we noted a global decrease in the levels of H3K27me3 in response to EzH2 knockdown by miR-101.

With constant progress in the understanding of mechanisms regulating the apoptotic process, it is becoming increasingly clear that miRNA may also operate through modulation of apoptosis (32). Our results clearly indicate that the increase in cell death observed with miR-101 re-expression is accompanied with an increase in the apoptotic cell population in EOC cell lines as evidenced by FACS analyses. We also observed an over-expression of pro-apoptotic *bak* and concomitant inhibition of the anti-apoptotic *bcl-2* gene expression with miR-101 re-expression.

Recent observations indicate that the depletion of EzH2 increases the expression of tumor suppressor genes (33). $P21^{waf1/cip1}$ is a tumor suppressor protein that binds to cyclin-CDK complexes and inhibits their catalytic activity, thus inducing cell cycle arrest at G1 to S phase (34). Loss of $p21^{waf1/cip1}$ expression is frequently observed in EOC and is correlated with a more aggressive form of the disease (35). ChIP analyses revealed that EzH2 knockdown by miR-101 re-expression inhibited the association of EzH2 with the $p21^{waf1/cip1}$ promoter, which could explain the increase in the expression of $p21^{waf1/cip1}$ observed on western blot. The increase in histone methylation at H3k27 in response to miR-101 re-expression, a mark of active euchromatin, further supports this observation. However, further research will be required to identify the molecular pathways involved in miRNA-activated gene expression and, specifically, the exact regions of methylation.

In addition to the *in vitro* tumor suppression seen with EzH2 knockdown by miR-101, our *in vivo* experiments indicate that miR-101 re-expression in EOC cells reduces their ability to form tumors in the SCID mouse xenograft model. Of note is the dramatic difference seen between *in vitro* and *in vivo* cell growth suppression. This can be explained by the fact that unlike the short duration of the *in vitro* experiments, mice were observed for 50 days after injection. The gene silencing effect of miR-101 is directly dependent on the number of molecules available in the cells. In cancer cells, miR-101 activity is short lived because the miR-101 molecules are reduced by half with each cell division. A possible solution would be a viral vector delivery system that circumvents this problem by creating sustained expression of miR-101 in target cells.

From a translational standpoint, this finding provides an exciting possibility for a novel target in EOC treatment. Indeed, miR-101 gene therapy can potentially supplement currently used chemotherapeutic agents in EOC, perhaps allowing for dose reductions and eventually leading to a decrease in side effects. However, the success of this combination therapy will ultimately depend on the ability to deliver the drug at the tumor site to mitigate any possible side effects. This remains a viable possibility, especially in EOC where the tumor is largely confined to the intra-peritoneal cavity and where spread to distant sites like the lungs and brain is not very common, allowing for effective intra-peritoneal delivery of treatment in advanced stage cancer. Experiments are underway in our laboratory to use Adeno-associated virus (AAV) as a vehicle for miR-101 intra-peritoneal delivery.

In summary, our results show, for the first time, that forced expression of miR-101 by a plasmid vector represents an efficient way of impairing cell proliferation and invasive potentials in EOC. In addition, we have provided a proof of principle that miR-101 inhibits the growth of EOC *in vitro* by up-regulating the tumor suppressor gene $p21^{waf1/cip1}$. Furthermore, demonstrating the *in vivo* ability of miR-101 re-expression to inhibit human xenografts in mice supports its potential role as a new modality for ovarian cancer treatment. Further studies on tumor tissue harvested from the experimental mice are underway in our lab, including Immuno-histochemical staining for $p21^{waf1/cip1}$ and miR-101 quantification by PCR to confirm the re-expression of $p21^{waf1/cip1}$ and the stability of the miR-101 transfection *in vivo*, respectively.

## REFERENCES


1. Jemal A, Siegel R, Ward E, Hao Y, Xu J, Thun M. Cancer statistics, 2009. CA: A Cancer J Clinicians. 2009;59:225.
2. McGuire W, Hoskins W, Brady M, Kucera P, Partridge E, Look K, *et al.* Cyclophosphamide and cisplatin compared with paclitaxel and cisplatin in patients with stage III and stage IV ovarian cancer. New Engl J Med. 1996;334:1.
3. Aghajanian C. Clinical update: novel targets in gynecologic malignancies, Vol. 31. Elsevier; 2004. p. 22–26.
4. Trimbosand J, Timmers P. Chemotherapy for early ovarian cancer. Curr Opin Obstet Gynecol. 2004;16:43.
5. Valencia-Sanchez M, Liu J, Hannon G, Parker R. Control of translation and mRNA degradation by miRNAs and siRNAs. Gene Dev. 2006;20:515.
6. Esquela-Kerscherand A, Slack F. OncomirsómicroRNAs with a role in cancer. Nat Rev Canc. 2006;6:259.
7. Calin G, Sevignani C, Dumitru C, Hyslop T, Noch E, Yendamuri S, *et al.* Human microRNA genes are frequently located at fragile sites and genomic regions involved in cancers. Proc Natl Acad Sci. 2004;101:2999.
8. Zhang L, Huang J, Yang N, Greshock J, Megraw M, Giannakakis A, *et al.* microRNAs exhibit high frequency genomic alterations in human cancer. Proc Natl Acad Sci. 2006;103:9136.
9. Lu L, Katsaros D, Rigault de la Longrais I, Sochirca O, Yu H. Hypermethylation of let-7a-3 in epithelial ovarian cancer is associated with low insulin-like growth factor-II expression and favorable prognosis. Canc Res. 2007;67:10117.
10. Dahiya N, Sherman-Baust C, Wang T, Davidson B, Shih I, Zhang Y, *et al.* MicroRNA expression and identification of putative miRNA targets in ovarian cancer. PLos One. 2008;3.
11. Friedman J, Liang G, Liu C, Wolff E, Tsai Y, Ye W, *et al.* The Putative Tumor Suppressor microRNA-101 Modulates the Cancer Epigenome by Repressing the Polycomb Group Protein EZH2. Canc Res. 2009;69:2623.
12. Varambally S, Cao Q, Mani RS, Shankar S, Wang X, Ateeq B, *et al.* Genomic loss of microRNA-101 leads to overexpression of histone methyltransferase EZH2 in cancer. Science. 2008;322:1695–9.
13. Malpica A, Deavers M, Lu K, Bodurka D, Atkinson E, Gershenson D, *et al.* Grading ovarian serous carcinoma using a two-tier system. Am J Surg Pathol. 2004;28:496.
14. Bachmann IM, Halvorsen OJ, Collett K, Stefansson IM, Straume O, Haukaas SA, *et al.* EZH2 expression is associated with high proliferation rate and aggressive tumor subgroups in cutaneous melanoma and cancers of the endometrium, prostate, and breast. J Clin Oncol. 2006;24:268–73.
15. Kleer CG, Cao Q, Varambally S, Shen R, Ota I, Tomlins SA, *et al.* EZH2 is a marker of aggressive breast cancer and promotes neoplastic transformation of breast epithelial cells. Proc Natl Acad Sci USA. 2003;100:11606–11.
16. Raman JD, Mongan NP, Tickoo SK, Boorjian SA, Scherr DS, Gudas LJ, *et al.* Increased expression of the polycomb group gene, EZH2, in transitional cell carcinoma of the bladder. Clin Canc Res. 2005;11:8570–6.
17. Varambally S, Dhanasekaran S, Zhou M, Barrette T, Kumar-Sinha C, Sanda M, *et al.* The polycomb group protein EZH2 is involved in progression of prostate cancer. Nature. 2002;419:624–9.
18. Krek A, Grün D, Poy MN, Wolf R, Rosenberg L, Epstein EJ, *et al.* Combinatorial microRNA target predictions. Nat Genet. 2005;37:495–500.
19. Reik W. Stability and flexibility of epigenetic gene regulation in mammalian development. Nature. 2007;447:425–32.
20. Wan M, Zweizig S, D'ablaing G, Zheng J, Velicescu M, Dubeau L. Three distinct regions of chromosome 6 are targets of loss of heterozygosity in human ovarian carcinomas. Int J Oncol. 1994;5:1043–8.
21. el-Deiry WS, Harper JW, O'Connor PM, Velculescu VE, Canman CE, Jackman J, *et al.* WAF1/CIP1 is induced in p53-mediated G1 arrest and apoptosis. Canc Res. 1994;54:1169–74.

22. Bandres E, Agirre X, Ramirez N, Zarate R, Garcia-Foncillas J. MicroRNAs as cancer players: potential clinical and biological effects. DNA Cell Biol. 2007;26:273–82.
23. Cumminsand J, Velculescu V. Implications of micro-RNA profiling for cancer diagnosis. Oncogene. 2006;25:6220–7.
24. Zhang B, Pan X, Cobb GP, Anderson TA, Zhang B, Pan X, *et al.* microRNAs as oncogenes and tumor suppressors. Dev Biol. 2007;302:1–12.
25. Iorio M, Visone R, Di Leva G, Donati V, Petrocca F, Casalini P, *et al.* MicroRNA signatures in human ovarian cancer. Canc Res. 2007;67:8699.
26. Taylorand D, Gercel-Taylor C. MicroRNA signatures of tumor-derived exosomes as diagnostic biomarkers of ovarian cancer. Gynecol Oncol. 2008;110:13–21.
27. Yang H, Kong W, He L, Zhao J, O'Donnell J, Wang J, *et al.* MicroRNA expression profiling in human ovarian cancer: miR-214 induces cell survival and cisplatin resistance by targeting PTEN. Canc Res. 2008;68:425.
28. Zhang L, Volinia S, Bonome T, Calin G, Greshock J, Yang N, *et al.* Genomic and epigenetic alterations deregulate microRNA expression in human epithelial ovarian cancer. Proc Natl Acad Sci. 2008;105:7004.
29. Strillacci A, Griffoni C, Sansone P, Paterini P, Piazzi G, Lazzarini G, *et al.* MiR-101 downregulation is involved in cyclooxygenase-2 overexpression in human colon cancer cells. Exp Cell Res. 2009;315:1439–47.
30. Chao-Wei C, Yi H, Ka-Wai L, Lih-Chyang C, Hua-Chien C, Shu-Jen C, *et al.* PKC alpha mediated induction of miR-101 in human hepatoma HepG2 cells. J Biomed Sci. 2040;17.
31. Cao Q, Yu J, Dhanasekaran S, Kim J, Mani R, Tomlins S, *et al.* Repression of E-cadherin by the polycomb group protein EZH2 in cancer. Oncogene. 2008;27:7274–84.
32. Calinand G, Croce C. MicroRNA signatures in human cancers. Nat Rev Canc. 2006;6:857–66.
33. Ougolkov A, Bilim V, Billadeau D. Regulation of pancreatic tumor cell proliferation and chemoresistance by the histone methyltransferase enhancer of zeste homologue 2. Clin Canc Res. 2008;14:6790.
34. Haradaand K, Ogden G. An overview of the cell cycle arrest protein, p21WAF1. Oral Oncol. 2000;36:3–7.
35. Schmider A, Gee C, Friedmann W, Lukas J, Press M, Lichtenegger W, *et al.* p21 (WAF1/CIP1) protein expression is associated with prolonged survival but not with p53 expression in epithelial ovarian carcinoma. Gynecol Oncol. 2000;77:237–42.